The Origin of Photoluminescence from α-Sexithienyl Thin Films

R. N. Marks, R. H. Michel, W. Gebauer, R. Zamboni,* and C. Taliani

Istituto di Spettroscopia Molecolare, Consiglio Nazionale delle Ricerche, Via P. Gobetti 101, 40129 Bologna, Italy

R. F. Mahrt and M. Hopmeier

Institut für Physikalische Chemie und Zentrum für Materialwissenschaften der Philipps Universität Marburg, Hans Meerwein Strasse, 35032 Marburg, Germany

Received: May 15, 1998; In Final Form: July 9, 1998

We have studied photoluminescence (PL) from sublimed films of α-sexithienyl (T6) in order to understand the nature of the excited species which give rise to radiative emission. Temperature-dependent measurements of the PL spectra show an apparent 530 cm^{-1} blue shift of the emission as the sample temperature decreases, and the integrated PL intensity at 50 K is 1 order of magnitude larger than that at 300 K. Time-resolved PL spectra (at 10 K) indicate a fast energy transfer of excitons to lower lying trap states on the time scale of 250 ps. Site-selective PL (SSPL) measurements made at 25 K show clearly that the peaks in the steady-state PL spectrum are not only due to vibronic structure, but to emission from different defect states. Emission from the highest energy peak disappears when the excitation energy is below 17700 cm^{-1}, and that from the second peak drops when the excitation is below 17095 cm^{-1}. PL excitation (PLE) measurements show absorption into a distribution of defect states at about 17700 cm^{-1}. Our data show that PL in T6 polycrystalline thin films originates from defect states. Comparison is made with the intrinsic excitonic PL of the T6 solid phase, demonstrating the relevance of defects in the radiative processes of rigid-rod-like conjugated systems.

Introduction

Conjugated organic materials have been studied for many years because of their novel optical and electronic properties, and currently organic light-emitting diodes (LEDs) and photodiodes are of great interest. For the understanding of the operation of these devices, the understanding of the nature of excited states in the active organic material is of fundamental importance, and this understanding is still debated among the scientific community. Unlike inorganic semiconductors, the primary product of photoexcitation is a bound electron−hole pair (a Frenkel exciton)[1] with a binding energy of typically few tenths of an electronvolt.[1−4] In the ordered solid-state excitons are mobile, with a diffusion length of few nanometers,[1,5] which results in efficient energy transfer to low-lying states. Photoluminescence (PL) or exciton dissociation will occur from these low-lying states, and a small number of trap states can therefore have a disproportionate effect both on PL and on the efficiency of generation of free carriers in a photodiode.[1]

We have performed a spectroscopic investigation of the states that give rise to PL in sublimed thin films of T6, a widely studied oligomer of interest as a model system for polythiophene and as active material in thin film transistors.[6−8] Vacuum sublimation may give rise to highly ordered films[7,9−13] whose morphology is determined primarily by the deposition rate, the substrate temperature during deposition, the amount of deposited material (i.e., thickness), and the angle of the substrate with respect to the impinging molecular beam. T6 films are polycrystalline, and on polar substrates such as quartz or indium tin oxide (ITO) the molecules align themselves at an angle of about 30° to the surface normal of the substrate.[7,9−11] The crystallite average size as determined by X-ray diffraction in films sublimed on the substrate kept at room temperature (rt) during deposition is about 30 nm.[7] Scanning force microscopy (SFM) measurements show that there is also a larger-scale structure in such films on the scale of 200 nm.[13] At higher deposition temperatures, the grain size (as measured by SFM technique) increases exponentially, reaching an average diameter of 1500 nm at 150 °C.[13] Because the first electronic transition of T6 is polarized parallel to the long molecular axis,[14,15] we may expect that the PL be polarized perpendicular to the basal plane of the film. On the contrary, measurements of electroluminescence and PL show that emission from films grown at rt is isotropic.[16,17] Only when the substrate temperature during deposition is raised above about 100 °C the emission becomes partially polarized, which also corresponds to the increased order in the morphology of the film.[16]

At an early stage of our work with light-emitting diodes made from T6 we observed a striking variation between the electroluminescence spectra of different diodes, nominally made in the same way. Moreover, we observed a similar behavior also for the PL spectra. We found that while the peak positions remained approximately constant between samples, the relative peak strengths varied widely. If the peaks were vibronic in origin, we would not expect any variance from sample to sample since the distribution of intensity between different vibronic levels in an optical transition is determined by the Huang−Rhys factor,[1] which is an intrinsic property of the molecule. This led us to consider the influence of defect states on the spectra of T6 films, as well as to consider more general effects of disorder and morphology on the excited states of conjugated organic materials.

Other work on T6 has also shown the importance of defect states. Photoluminescence from ultrathin films of T6 has been

S1089-5647(98)02250-0 CCC: $15.00 © 1998 American Chemical Society
Published on Web 09/09/1998

found to show a much higher degree of fine structure than can be seen in conventional films on the order of 100 nm thick.[18] In single crystals of T6, the emission spectrum depends strongly on crystal quality. Early work showed defect states PL emission even at 4.2 K,[19] whereas in high quality crystals of T6 now available, evidence of emission from bulk excitons at temperature below 50 K has been found.[20] This paper presents a detailed spectroscopic analysis of T6 thin films in order to clarify the origin of their PL.

Experimental Section

Films of T6 were sublimed both in ultrahigh vacuum (UHV) using an organic molecular beam deposition system (OMBD)[21] as well as in high vacuum from a quartz crucible onto substrates held at about 10 cm from the sublimation source. Quartz and ITO substrates were used. ITO is an interesting substrate because it is commonly used as the hole injecting electrode in LEDs. The morphology of the film can be modified changing the deposition conditions.

The substrate temperature and the rate of deposition are expecially important. In these experiments the rate of evaporation was kept below 5 nm/s, and the substrate temperature was varied between rt and 150 °C.

The sample was mounted in a coldfinger cryostat, and the sample temperature was varied down to a nominal temperature of about 12 K. Because the sample is not in contact with the liquid helium, its actual temperature was about 25 K. For the PL and site-selective PL (SSPL) experiments, spectra were measured with a Hamamatsu PMA-11 optical multichannel analyzer fitted with a CCD array, with the sample excited by a laser. PL measurements were made either by exciting T6 with an Ar^+ laser lines, or with a Nd:YAG pumped dye laser (the latter was used for the SSPL measurements). The excitation source for the PLE measurements was the output of a 0.25 m monochromator with a tungsten lamp source. The source was chopped to allow a lock-in detection technique to be used. The PL was focused onto a 0.20 m monochromator which was used to select the spectral window of detection. An RG928 photomultiplier tube was used to detect the signal at the chosen wavelength. The output from the photomultiplier was amplified by a current-to-voltage amplifier, and then detected with a lock-in technique. The time-resolved PL measurements were done using as an excitation source a pulsed laser beam (100 fs) at 3.1 eV derived from a frequency-doubled mode-locked Ti: sapphire laser. The PL decay was monitored by a streak camera with a time resolution of 6 ps.

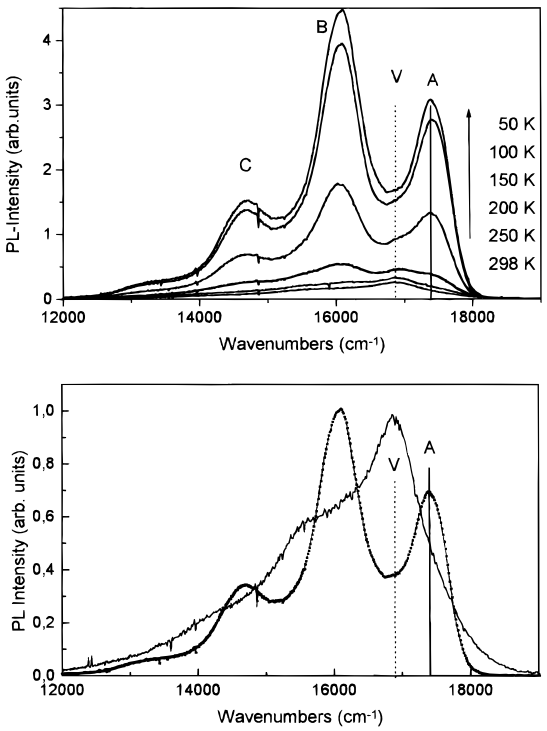

Figure 1. (a) The temperature dependence of PL from a film of T6 sublimed in high-vacuum. Vertical lines and letters select particular peaks and spectral positions (see text). (b) The 50 and 298 K PL spectra shown together, normalized to a maximum signal of unity. Vertical lines and letters select particular peaks and spectral positions (see text)

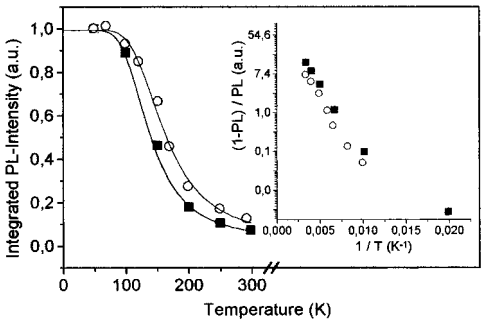

Figure 2. The temperature dependence of the quantum efficiency of PL in two high-vacuum sublimed films of T6. Open circles indicates a film sublimed at a substrate temperature of 28 °C, whereas the full squares a film sublimed at a substrate temperature of 150 °C. The fitting of the two curves are made with the equation $\eta=1/(1 + Ce^{-E_a/k_bT})$, where η is the relative PL efficiency and C is a constant. The inset shows an Arrhenius plot of the experimental data.

Results

The temperature evolution of the PL spectrum of a high-vacuum sublimed T6 film on ITO kept at rt during deposition, is shown in Figure 1a. Figure 1b shows the PL spectra at 298 and 50 K, respectively, normalized to a peak intensity of unity. The integrated intensity of the PL increase by about 1 order of magnitude when the sample is cooled (Figure 2), and there is an apparent blue shift of the first maximum of about 530 cm^{-1}. This evidence suggests the appearance of new peaks activated by temperature which dominate the emission spectrum at the lowest temperatures, rather than to a shift in the PL spectrum. This can be seen most clearly considering the spectrum taken at 200 K (Figure 1a), in which the spectral features of the room temperature and of the 50 K spectra are both present, labeled as features V and A, respectively. At 50 K a shoulder is visible at about 16900 cm^{-1}, which probably corresponds to the peak V seen at this position at room temperature (see Figure 1b). It is noteworthy that the low-temperature spectral features reported in ref 18 are in excellent agreement with our spectra. We have found the same phenomenon both in films grown with the substrate held at room temperature and in films grown at 150 °C.

We have labeled the features of the low-temperature PL spectrum of T6 as peaks A, B, C, and V as show in Figure 1a,b. The origin of the different peaks will be elucidated in the following sections. Figure 2 shows the evolution of the PL intensity with sample temperature for films grown at deposition temperature equal to rt and 150 °C, respectively. The PL efficiency was normalized to unity at the lowest temperature point (50 K). From rt down to about 50 K, the yield increases exponentially, and then levels off at an almost fixed value. This

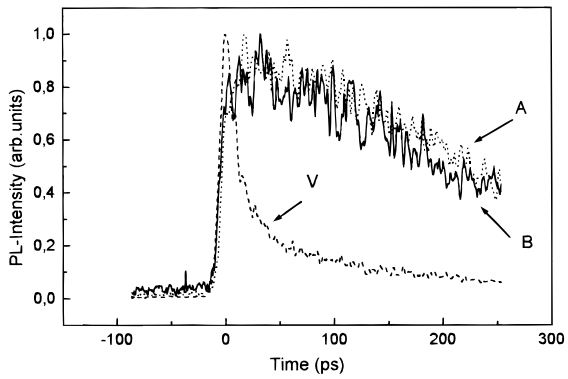

Figure 3. The transient response of PL as a function of the detection energy. Solid line, 17550 cm^{-1}; dotted line, 16250 cm^{-1}; dashed line, 16900 cm^{-1}. Capital letters mark the spectral position as indicated in Figure 1 and into the text.

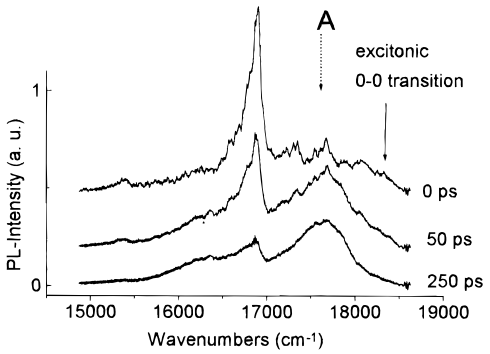

Figure 4. Transient PL spectra of a T6 film, taken between 0 and 250 ps after excitation. The dotted arrow mark the positon of peak A as indicated in Figure 1 and the full line arrow mark the 0−0 excitonic origin (see text).

change in PL efficiency reflects the change in the PL spectra described above, suggesting that they are closely linked phenomena.

The temperature dependence of the PL efficiency η is well fitted with by the function $\eta = 1/(1 + Ce^{-E_a/k_bT})$ where C is a constant. This functional form mirrors the existence of two competitive decay channels. The curve fits give activation energies $E_a \cong 60$ meV, for both the T6 films grown on the substrate at rt and at 150 °C. The inset in Figure 2 shows an Arrhenius plot of the experimental data making more clear the actived nature of the process.

We have performed time-resolved measurements of the PL in T6 films at 10 K to study the emission in more detail. The lifetime of the PL at 17550 ± 80 cm^{-1} (peak A), 16900 ± 80 cm^{-1} (peak V), and 16250 ± 80 cm^{-1} (peak B), is shown in Figure 3. The PL at peak A and B has a lifetime of 750 ps and is quite well fitted by a single exponential decay. In contrast the decay of the PL at peak V is nonexponential, decaying at more than 50 ps initially and only later slowing down to 750 ps. Figure 4 show the spectrum of PL from this film at different times after excitation (0, 50, and 250 ps time delay). At zero time after excitation, the PL spectrum shows a fine structure and reflects the spectral features found in high quality T6 single crystals.[20] The transient spectrum only begins to resemble that of the steady-state after about 250 ps, where the peak A became dominant and the fine structure disappears.

Figure 5 shows the SSPL measurements, that is, the PL spectrum of a T6 film grown in UHV as a function of the excitation wavelength. These measurements were taken with the sample at about 25 K. The top curve (curve a) shows the

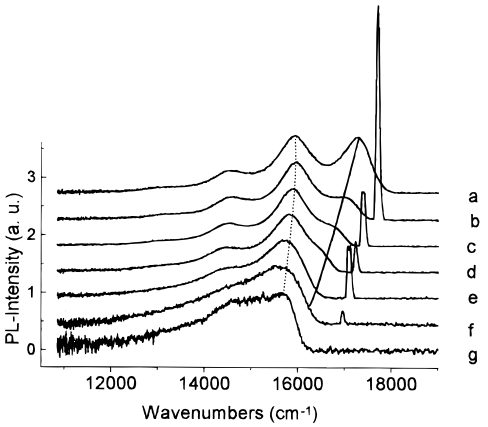

Figure 5. Site-selective photoluminescence (SSPL) measurements of a T6 film. The excitation energies were: (a) 20490 cm^{-1}, (b) 17860 cm^{-1}, (c) 17700 cm^{-1}, (d) 17390 cm^{-1}, (e) 17240 cm^{-1}, (f) 17095 cm^{-1}, (g) 16950 cm^{-1}. In scans b−f the sharp high-energy peak is the laser excitation line. Dotted and full lines are an eye guide for the spectral evolution of the marked PL peaks

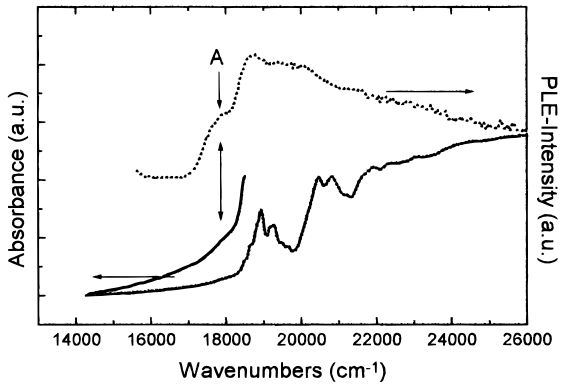

Figure 6. Photoluminescence excitation (PLE) spectrum of a T6 film for detection energies of 15385, 15875, 16665, and 17300 cm^{-1}. The four detection energies show the same PLE spectrum (up dotted curve). A normalized absorption spectrum (short-dashed lower curve) of T6 is shown for comparison. The vertical double arrow marks the correspondence between the low energy PLE peak and the weak shoulder in the absorption spectrum (middle full curve magnified × 4). The capital letter A marks the spectral position of the defect peak discussed in the text.

spectrum when exciting at 20490 cm^{-1}. This spectrum does not start to change until the excitation energy reaches about 17700 cm^{-1} (curve c). Because the excitation energy is scanned from 17700 cm^{-1} (curve c) to 17390 cm^{-1} (curve d), peak A in the PL spectrum (initially at about 17280 cm^{-1}) shifts to the red and largely disappears. Peaks B and C are still visible although the peak A has disappeared, and both their position and relative intensity remain fairly unchanged. At excitation energies lower than about 17260 cm^{-1} (curve f and g) the peak B and C change shape and relative intensity.

We also performed PLE measurements to search for low-lying states at the absorption edge of the T6. Figure 6 shows the spectrum we obtained with the same UHV film used above, at temperature of about 25 K, for detection energies of 15385, 15875, 16665, and 17300 cm^{-1}. All four detection energies gave rise to the same PLE spectrum, that is, the PLE spectrum is essentially independent of the detection wavelength. The rise in the curves at the lowest energy is due to light leakage through the final monochromator as the excitation energy approaches that of the detection window. An absorption spectrum of a similar film, taken at about 5 K, is shown for comparison.

There is a lot of fine structure in the absorption spectrum, similar to that of single crystals,[19,20] indicating the film is highly crystalline. However, while there is a very strong peak in the PLE spectrum at about 17700 cm^{-1}, there is only a weak shoulder in the tail of the onset of the absorption spectrum at this energy, indicating the defect origin of the peak at 17700 cm^{-1} in thin films.

Discussion

The time-resolved measurements of Figures 3 and 4 prove that the low-temperature emission at 16900 cm^{-1} (peak V) arise from two different excited species. The PL lifetime at this energy has two components (50 and 750 ps), whereas at other energies there is a single lifetime of about 750 ps. The spectrum of this short-lived emission can be seen clearly in Figure 4, in which the zero-time PL spectrum shows a fine structure and the low-temperature steady-state PL peak A only begins to dominate after about 250 ps. This lead us to believe that energy transfer occurs from the exciton band, which give rise to the zero-time PL signal, to defect states in the film which are responsible for the broad steady-state PL. Moreover, our SSPL measurements (Figure 5) show that the low-temperature steady-state PL spectrum cannot only be explained in terms of emission from a single excited state with associated vibronic progression of the C═C stretching mode. In fact, as the excitation energy is varied between 17855 and 17240 cm^{-1}, the intensity of the peak A falls and shifts toward lower energies while the other two main peaks B and C in the PL spectrum are completely unaffected (both their position and relative intensity remain unchanged). This demonstrates quite clearly that the states which give rise to the emission at peak A are different to those which give rise to peak B and below.

Because peak A red shifts and disappears at excitation energies between about 17860 and 17240 cm^{-1}, we infer that this latter energy corresponds to the tail of the distribution of states that give rise to this emission band. The PLE spectrum of Figure 6 shows that there is a broad distribution of defect states below the absorption manifold, centered at about 17700 cm^{-1}, which we therefore identify as the states which give rise to the emission of peak A. When the excitation energy drops lower than 17095 cm^{-1}, peaks B and C change their relative intensity and shape, suggesting emission from different sets of defect states. However, in PLE only one defect peak (i.e., the peak A) can be seen (Figure 6), and the spectrum is *independent of* the energy of the detection window. Remarkably, as marked in Figure 6 by a double arrow the one-photon absorption spectrum shows a shoulder at the same energy of the PLE defect states peak A indicating a rather large density of state for this particular defects distribution. This implies that the density of states of the defects that give rise to emission at peaks B and C, located at low energy, are too low to be seen in this PLE measurement. Nevertheless, these levels can be populated directly by SSPL (see Figure 5) and there is efficient energy transfer migration from the first defect band at 17700 cm^{-1} (peak A) to those at lower energies. As a result of this energy transfer, excitation into the first defects distribution A also results in emission from the lower lying defect states.

The temperature dependence of the PL spectrum in T6 films (Figure 1a,b) suggests that at different temperatures emission occurs from different species within the film. At low temperature there is mainly emission from species that give rise to the peaks A, B, and C, whereas at room temperature three different peak positions appear in the PL spectrum (see Figure 1b). Figure 7 shows the time-resolved PL spectrum of T6 at zero time (measured at 10 K), together with the steady-state PL spectra at low temperature and room temperature. Comparison of this time-resolved spectrum with the room-temperature spectrum suggests emission from the same excited state. Remarkably, the time-resolved spectrum at zero-time delay has its origin at 18350 cm^{-1} together with the vibronic progression that was found and assigned in ref 20 by absorption and PL spectroscopy on T6 single crystals.

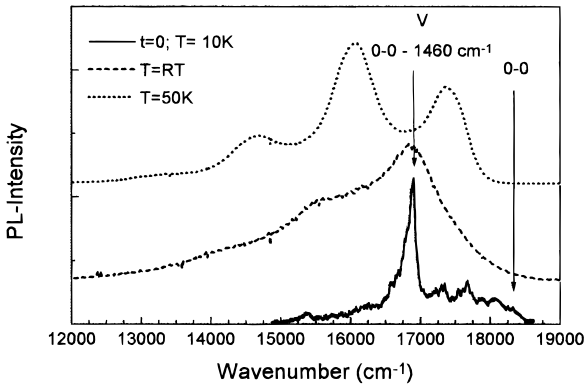

Figure 7. Time-resolved PL at zero delay and at 10 K (full line) and steady-state PL at room temperature (dashed-line) and at 50 K (dotted line) of a T6 thin film. Both 0−0 excitonic origin and the most intense vibronic peak V are indicated.

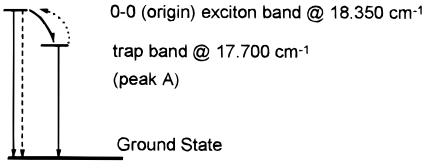

Figure 8. Schematic diagram of the temperature activated de-trapping process from the defect distribution of states (peak A) to the 0−0 exciton origin of vacuum sublimed T6 thin films. The calculated activation energy of about 60 meV fits well with the energy difference between the above metioned 0−0 (18350 cm^{-1}) and the peak A (17700 cm^{-1}).

The steady-state PL at low temperature shows a different spectrum compared to the others in Figure 7, having the peaks previously labeled A, B, and C. SSPL (Figure 5) and PLE (Figure 6) has shown that these are not due to a vibronic progression from an allowed origin, but rather to emission from different defects states. The temperature dependence of the PL, which follows an exponential relationships, indicates an activated two-channel process with an activation energy of about 60 meV (500 cm^{-1}). This activation energy is independent of the substrate temperature during deposition of the film in the range from room temperature up to about 150 °C, and therefore is also independent of the morphology of the films.[13,16,17]

The activation energy of 500 cm^{-1} is comparable with the difference between the dominating distribution of defect states (giving rise to PL peak A at 17700 cm^{-1}) and the excitonic origin located at 18350 cm^{-1}. We suggest, therefore, that a key process in PL in these films is the trapping of excitons in this defect band. At low temperatures the steady-state PL is from these and lower lying defects, while time-resolved measurements indicate that at short times after excitation excitonic emission dominates. As the temperature rises detrapping from this defect band becomes important, giving rise to room-temperature PL from excitons, with a spectrum that is more similar to the excitonic emission from high-quality single crystals. A schematic representation of the process is shown in Figure 8. This interpretation is also consistent with other measurements on PL in T6 thin films reported by other

groups,[18,22−24] where a complete analysis and a comprehensive interpretation of the PL mechanism have not been carried out. However, the nature of the defects that give rise to the low-energy PL component is still an open question. To disentangle how the solid phase of T6 forms systematically reproducible defect states that give rise to a PL component that dominates the radiative emission it is necessary to further investigate and understand how to control the structure and the ordering during the growth of thin films.

Conclusions

Our results show that the low-temperature PL of sublimed polycrystalline thin films of T6 is dominated by radiative emission from defects states. As the temperature rises thermally activated detrapping becomes important, and the room-temperature emission is excitonic. We have also identified the 0−0 origin of PL and its excitonic nature. This origin is located at 18350 cm^{-1} and there is an associated vibronic progression. Time-resolved PL measurements show that energy transfer occurs from the PL origin into defect states that dominate the PL spectrum after 250 ps. SSPL indicates the presence of at least three defects states and PLE shows that there is one dominant defect states distribution just below the absorption edge. The nature of those defect states is not elucidated by our experiments. Nevertheless, from the behavior of the investigated spectroscopic observable, we believe that they are connected to the molecular packing during the solid phase formation of the thin film.

Thin films are of utmost importance and are commonly used for application related to the unique properties of conjugated organic materials. The presence of defect states determine the fate of excitations in the film. Although these results are specific to T6, most sublimed molecular films are polycrystalline, and we expect that defect states will play as important a role in other conjugated molecular materials as they do in T6.

Acknowledgment. Valuable discussion with Prof. H Bässler and Prof. W. W. Rülhe, Dr. F. Biscarini, Dr. M. Muccini, and Dr. G. Ruani are gratefully acknowledged. The temperature-dependent measurements of PL were performed in Prof. R. H. Friend's group in the Cavendish Laboratory, Cambridge, U.K. This work was performed as a part of the European Union Esprit project LEDFOS and as a part of the European Union TMR project SELOA. R.F.M. gratefully acknowledges financial support by Deutsche Forschungsgemeinschaft. We thank Hamamatsu Photonics Italia for financial support of the PMA-11 optical multichannel analyzer.

References and Notes

(1) Pope, M.; Swenberg, C. E. *Electronic Processes in Organic Crystals*; Clarendon: Oxford, 1982.
(2) da Costa, P. G.; Conwell, E. M. *Phys. Rev. B* **1993**, *48*, 1993.
(3) Shuai, Z.; Brédas, J. L.; Su, W. P. *Chem. Phys. Lett.* **1994**, *228*, 301.
(4) Brédas, J. L.; Cornill, J.; Heeger, H. J. *Adv. Mater.* **1996**, *8*, 447.
(5) Halls, J. J. M.; Pichler, K.; Friend, R. H.; Moratti, S. C.; Holmes, A. B. *Appl. Phys. Lett.* **1996**, *68*, 3120.
(6) Garnier, F.; Horowitz, G.; Peng, X.; Fichou, D. *Adv. Mater.* **1990**, *2*, 592.
(7) (a) Ostoja, P.; Guerri, S.; Rossini, S.; Servidori, M.; Taliani, C.; Zamboni, R. *Synth. Metals* **1993**, *54*, 447. (b) Ostoja, P.; Guerri, S.; Impronta, M.; Zabberoni, P.; Danieli, R.; Rossini, S.; Taliani, C.; Zamboni, R. *Adv. Mater. Opt. Electron.* **1992**, *1*, 127.
(8) Dodabalapur, A.; Torsi, L.; Katz, H. E. *Science* **1995**, *268*, 270.
(9) Servet, B.; Ries, S.; Trotel, M.; Alnot, P.; Horowitz, G.; Garnier, F. *Adv. Mater.* **1993**, *5*, 461.
(10) Porzio, W.; Destri, S.; Mascherpa, M.; Brückner, S. *Acta Polym.* **1993**, *44*, 266.
(11) Porzio, W.; Destri, S.; Mascherpa, M.; Rossini, S.; Brückner, S. *Synth. Metals* **1993**, *55*, 408.
(12) Servet, B.; Horowitz, G.; Ries, S.; Lagorsse, O.; Alnot, P.; Yassar, A.; Deloffre, F.; Srivastava, P.; Hajlaoui, R.; Lang, P.; Garnier, F. *Chem. Mater.* **1994**, *6*, 1809.
(13) Biscarini, F.; Zamboni, R.; Samorì, P.; Ostoja, P.; Taliani, C. *Phys. Rev. B* **1995**, *52*, 14868.
(14) Lazzaroni, R.; Pal, A. J.; Rossini, S.; Ruani, G.; Zamboni, R.; Taliani, C. *Synth. Metals* **1991**, *42*, 2359.
(15) Dippel, O.; Brandl, V.; Bässler, H.; Danieli, R.; Zamboni, R.; Taliani, C. *Chem. Phys. Lett.* **1993**, *216*, 418.
(16) Marks, R. N.; Biscarini, F.; Zamboni, R.; Taliani, C. *Europhys. Lett.* **1995**, *32*, 523.
(17) Marks, R. N.; Biscarini, F.; Virgili, T.; Muccini, M.; Zamboni, R.; Taliani, C. *Philos. Trans. R. Soc. London A* **1997**, *355*, 763.
(18) Gebauer, W.; Väterlein, C.; Soukopp, A.; Sokolowski, M.; Hock, R.; Port, H.; Bäuerle, P.; Umbach, E. *Synth. Metals* **1997**, *87*, 127.
(19) Muccini, M.; Lunedei, E.; Taliani, C.; Garnier, F.; Bässler, H. *Synth. Metals* **1997**, *85*, 600.
(20) a) Muccini, M.; Lunedei, E.; Bree, A.; Horowitz, G.; Garnier, F.; Taliani, C. *J. Chem. Phys.* **1998**. In press. (b) Marks, R. N.; Muccini, M.; Lunedei, E.; Michel, R.; Murgia, M.; Zamboni, R.; Taliani, C.; Horowitz, G.; Garnier, F.; Hopmeier, M.; Oestreich, M.; Mahrt, R. F. *Chem. Phys.* **1998**, *227*, 49.
(21) Zamboni, R.; Muccini, M.; Kapousta, O.; Murgia, M.; Abbate, F.; Lunedei, E.; Taliani, C.; Kajzar, F. *Proceedings of SPIE, Fullerenes and photonics III* **1996**, *2854*, 182.
(22) Deloffre, F.; Garnier, F.; Srivastava, P.; Yassar, A.; Fave, J. L. *Synth. Metals* **1994**, *67*, 223.
(23) Yassar, A.; Horowitz, G.; Valat, P.; Wintgens, V.; Hmyene, M.; Deloffre, F.; Srivastava, P.; Lang, P.; Garnier, F. *J. Phys. Chem.* **1995**, *99*, 353.
(24) Oelkrug, D.; Egelhaaf, H.-J.; Worall, D. R.; Wilkinson, F. *J. Fluores.* **1995**, *5*, 165. Also see: Egelhaaf, H.-J. Ph.D. Thesis, University of Tübingen, 1996.